13th World Conference on Earthquake Engineering
Vancouver, B.C., Canada
August 1-6, 2004
Paper No. 370

EVALUATION OF ULTIMATE DEFORMATION CAPACITY AT AXIAL LOAD COLLAPSE OF REINFORCED CONCRETE COLUMNS

Hassane OUSALEM[1], Toshimi KABEYASAWA[2] and Akira TASAI[3]

SUMMARY

While collapse vulnerability of reinforced concrete building frames constructed prior modern seismic codes' introduction has been well documented by earthquake reconnaissance, the mechanisms leading to collapse are not well understood. Identification of such processes is of importance.

Two series of tests were conducted on scaled reinforced concrete columns. In the first series, lateral loading was common for all specimens. Selected parameters were concrete strength and applied axial load: constant and varying ones. In the second series, axial load was common for all specimens. Selected parameters were shear span ratio, transverse reinforcement ratio and lateral loading simulating: near and far field earthquakes. Results from the first test series concluded that axial load type and magnitude affect columns' lateral deformation capacity, shear degradation and axial stiffness. Results from the second series concluded that lateral loading type has, in some cases, no influence on the lateral or axial deformability of columns, especially when the amount of transverse reinforcement is low. Therefore, in some other cases, shear strength evolution is affected by lateral loading type.

An analytical study based on the experimental results was carried out to estimate the lateral drift at axial load collapse. The analysis suggested a simple formulation as a function of the design parameters of columns and axial load levels. The proposed formulation is considered as a lower limit response that columns may fulfill.

INTRODUCTION

To sustain applied loads during seismic shakings, structural elements in moderately tall buildings, particularly reinforced concrete frames, have performed differently according to their geometric, materials and loading characteristics. Different failure modes and collapses have been mentioned in the literature, which were then related to different parameters and causes. These parameters and their combinations have taught the concerned community about the expected seismic performance of structural elements and how to improve it in case of both planned or existing structures. Consequently, different conclusions were drawn and recommendations were advised. While seismic performance of columns was

[1] Ph.D. Candidate, The University of Tokyo, Japan. Email: oushas@eri.u-tokyo.ac.jp
[2] Professor, Earthquake Research Institute, University of Tokyo, Japan. Email: kabe@eri.u-tokyo.ac.jp
[3] Associate Professor, Yokohama National University. Email: tasai@arc.ynu.ac.jp

considered for different reasons inadequate beyond certain level of damage or lateral strength decay, some damaged structural elements or whole partially damaged structures were condemned to collapse though they were still withstanding vertical loads. Although collapse vulnerability of reinforced concrete building frames constructed prior to the introduction of modern seismic codes has been well documented by earthquake reconnaissance, the mechanism that lead to collapse are still not well understood.

For life safety purposes, for economic reasons and for monitoring of the existing construction patrimony, different views emerged as to the way to deal with such damaged cases and to evaluate their ultimate deformation capacities at axial load collapse and some experimental tests were conducted, for example Moehle [1], Takaine [2], Uchida [3] and Ousalem [4, 5]. Actually, assessment and evolution of strength and stiffness of existing or newly designed critical reinforced concrete structures and evaluation of their performance under various loading, especially at very advanced stage of damage, strongly requires a well understanding of the phenomena affecting the behavior of these structures and all their individual components, Kwak [6].

To a better understanding as to ultimate capacity limit, particularly for columns failing in shear, two series of tests were conducted on one-third scaled square-cross-section reinforced concrete columns. Effects of different parameters on columns' responses were investigated and their results are presented. Also, a simple formulation based on test results is suggested.

EXPERIMENTAL INVESTIGATION

Tested specimens

To investigate the capacity limit relationship "lateral deformation-axial load", particularly for columns failing in shear, two series of tests were conducted on one-third scaled square-cross-section reinforced concrete columns, simulating columns existing in the first story of moderate tall buildings. Fig.1 and Table 1 illustrate characteristics of tested columns. Columns were loaded simultaneously in the axial and lateral directions. Laterally, columns were subjected to an anti-symmetric double curvature bending where loading path was controlled by displacement. Generally, tests on reinforced concrete columns are concluded soon after reaching shear failure, though tested columns still possess a certain residual capacity to sustain applied axial loads. These tests went beyond the shear failure of columns till they collapsed under vertical loads.

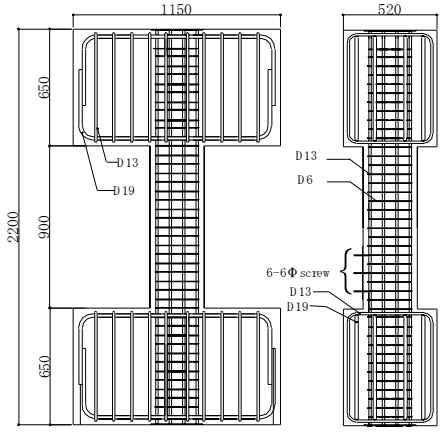

Fig.1 Geometric details of one of tested specimens

In the first series (2001), while lateral loading was the same for all specimens (loading Type-1 in Fig.2), applied axial load was constant for some specimens and varying for others (Fig.3). Varying axial load N was proportional to the applied lateral force Q according to Equation 1.

$$N = N_0 + \alpha Q \quad (1)$$

where N_0 is the initial compressive force and α the axial load factor, taken as 4.5 simulating the varying axial load in a medium-rise building. The selected parameters were concrete strength and applied axial load.

In the second series (2002), while axial load was the same for all specimens (Fig.3), lateral loading was of two types. Few hysteretic reversals loading (Type-3) with large peaks and monotonic phase simulated near field earthquakes and many hysteretic reversals loading (Type-2) with increasing small peaks simulated far field earthquakes. The selected parameters were shear span ratio, transverse reinforcement ratio and lateral loading.

Table 1 Characteristics of tested specimens

Specimen	b (mm)	D (mm)	a (mm)	S_t (mm)	ρ_{ls} (%)	ρ_{ws} (%)	f_{ly} (MPa)	f_{wy} (MPa)	F_c (MPa)	N_0 (kN)	Lat. Load
Test 2001											
C1	300	300	450	160	1.693	0.083	340	587	13.5	364.5C	type-1
C4	300	300	450	75	1.693	0.284	340	384	13.5	364.5C	type-1
C6	300	300	450	75	1.693	0.284	340	384	13.5	243.0V	type-1
C8	300	300	450	75	1.693	0.284	340	384	18.0	486.0C	type-1
C10	300	300	450	75	1.693	0.284	340	384	18.0	243.0V	type-1
C12	300	300	450	75	1.693	0.284	340	384	18.0	324.0C	type-1
Test 2002											
D1	300	300	300	50	1.693	0.43	447	398	27.7	540.0C	type-2
D16	300	300	300	50	1.693	0.43	447	398	26.1	540.0C	type-3
D11	300	300	450	150	2.258	0.14	447	398	28.15	540.0C	type-2
D12	300	300	450	150	2.258	0.14	447	398	28.15	540.0C	type-3
D13	300	300	450	50	2.258	0.43	447	398	26.1	540.0C	type-2
D14	300	300	450	50	2.258	0.43	447	398	26.1	540.0C	type-3
D15	300	300	450	50	2.258	0.85	447	398	26.1	540.0C	type-3

Notation: b= section's width, D= section's height, a= shear span (half of column height), S_t= stirrups spacing, ρ_{ls}= total longitudinal reinforcement ratio, ρ_{ws}= transverse reinforcement ratio, f_{ly}= longitudinal reinforcement yield strength, f_{wy}= transverse reinforcement yield strength, F_c= concrete strength, N_0= initial axial load, C= constant axial load, V= varying axial load, type-1 & type-2= simulation of far field earthquake, type-3= simulation of near field earthquake.

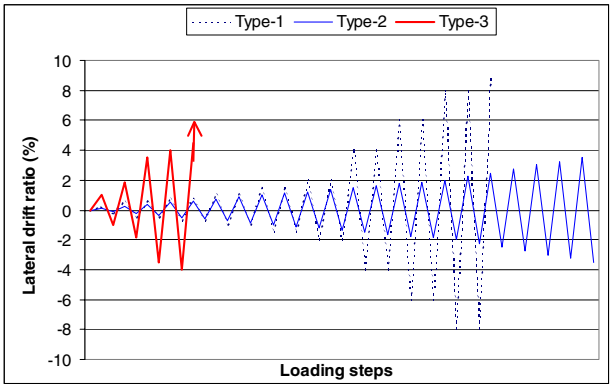

Fig.2 Lateral loading patterns

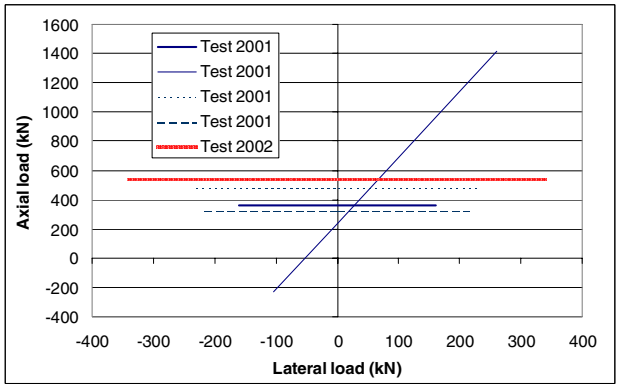

Fig.3 Axial loading patterns

Columns responses and observations

Response of columns to different combined loadings varied according to loadings magnitude, axially or laterally, slenderness, reinforcement content and material characteristics. Fig.4 and Fig.5 illustrate, respectively, 2001 tests and 2002 tests responses of some columns in terms of lateral load and lateral drift. Fig. 6 encloses the spread results in terms of applied axial load ratio ($\eta = N/(bDF_c)$), maximum attained lateral drift ratio (R), and axial deformation at collapse of all tested specimens.

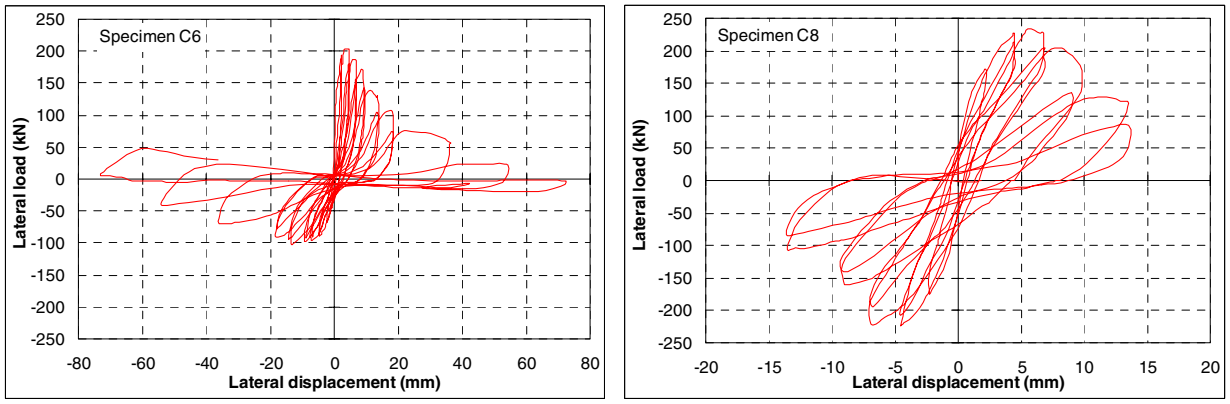

Fig.4 Lateral load – lateral drift response of some columns from experimental test of 2001

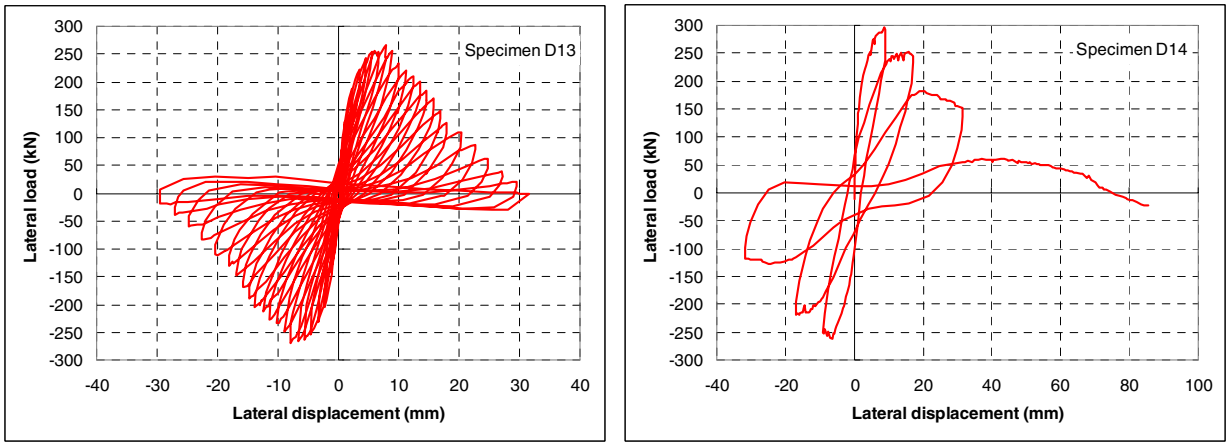

Fig.5 Lateral load – lateral drift response of some columns from experimental test of 2002

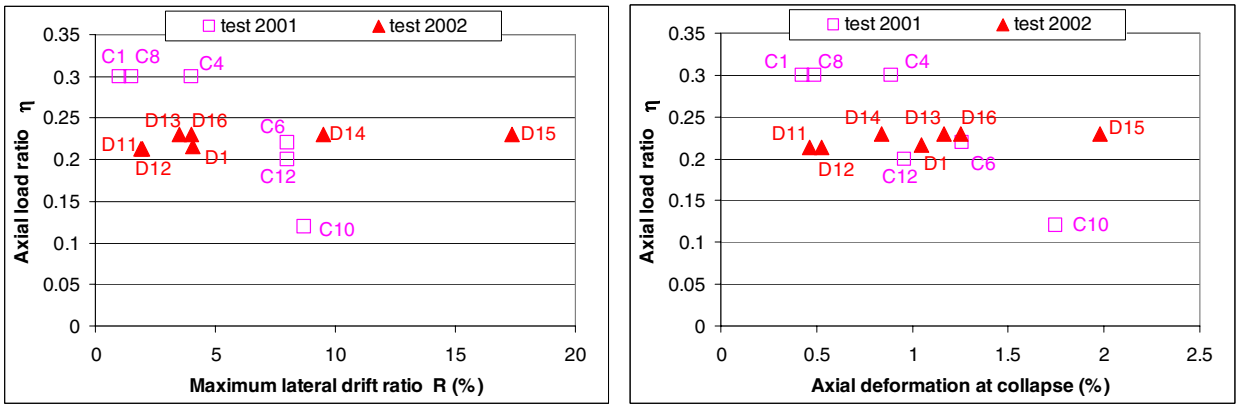

Fig.6 Performance of tested specimens

All specimens in both series were designed to fail in shear soon before or after yielding, except one element in the second series, specimen D15, which was expected to fail in flexure. Although some noticed differences between the assumed concrete strength and the actual strength at casting, almost all columns failed as predicted by design. Data analysis indicated the dominance of shear deformation during loading as to the flexure deformation. Curvature-lateral drift response curves of all specimens, except specimen D15, showed a fast increase in the lateral deformation rather than in the curvature. In the first series, specimens C1, C4 and C8 experienced clear tension shear failures, and specimens C6, C10 and C12 experienced truss mechanism failures. In the second series, specimens D1, D16, D11 and D12 experienced clear tension shear failures, and specimens D13 and D14 experienced truss mechanism failures. Table 2 illustrates a part of results of tested columns.

Observations made on both series' tested specimens identified that for all columns cracking pattern influenced very much behavior of specimens, shear degradation, stiffness changes and was a crucial indicator that conditioned failure mode and collapse. Collapse took place when columns were unable to sustain any more the applied axial loads, which corresponded at the time when shear strength decay consumed nearly the whole lateral capacity of columns. Collapse took place, in most cases, under reversals within peaks, however in few cases it occurred at peaks or at maximum attained lateral displacement when lateral loading reached a monotonic path, as mentioned by a diamond sign in Table 2. Actually, the collapse occurred along inclined planes at different angles, depending on material characteristics and loading levels. It was noticed that axial load level and amount of stirrups have a strong influence on the plane inclination, especially when axial load varied. In the contrary, lateral loading type has less influence on rupture plane inclination. Observed inclination angles as to the vertical axis of columns are presented in Table 2. The angles were assessed subjectively according to the judgment of the observer during testing of specimens and avoidable slight errors of evaluation are not drawn aside.

Table 2 Compiled results from 2001 and 2002 experimental tests

Specimen		δ_s (mm)	δ_m (mm)	Q_t (kN)	θ (degree)
2001	C1	7.09	9.06	160.4	21.5
	C4	9.07	36.24	171.1	22.0
	C6	8.99	72.13	203.9	47.5
	C8	9.65	13.64	233.0	24.0
	C10	11.33	78.28	262.1	50.0
	C12	13.50	72.64	217.1	47.0
2002	D1	5.84	24.33	341.1	40.7
	D16	8.32	24.02	341.6	38.0
	D11	7.92	16.95	242.8	24.1
	D12	9.81	17.46	250.4	18.5
	D13	12.41	31.52	266.1	39.0
	D14	16.95	90.50 ◊	296.1	33.0
	D15	32.10	161.00 ◊	327.9	*

Notation: δs= lateral displacement at shear failure (20% loss Q_t), δm= achieved maximum lateral displacement, Q_t= maximum shear strength from test, θ= observed failure plane inclination, *= Specimen D15 failed in flexure and is not included, ◊= achieved maximum lateral displacement corresponds to collapse

Tests conclusions

Analysis of experimental results of the first series concluded that higher axial loads induce steeper failure planes and higher axial load ratios induce lower lateral deformations. When compared to constant axial loads, varying axial loads allow larger deformations and lower shear degradation and this fact is enhanced

for higher concrete strength. Also, column axial stiffness degradation is lower under varying axial loads than under constant axial loads.

Analysis of experimental results of the second series concluded that few hysteretic reversals loadings induce slightly steeper failure planes than many hysteretic reversals loadings. Higher lateral deformability is reached for columns with high transverse reinforcement ratios or high shear span ratio under few hysteretic reversals. Also, for low transverse reinforcement ratios, lateral loading type has a negligible influence on the maximum attained lateral deformability, however, while maximum shear strength is almost the same on the first loading direction for loading types, on the opposite loading direction the maximum shear strength is higher under few hysteretic reversal loading than under few reversal loading. Shear strength degradation is lower under few hysteretic reversals than under many hysteretic reversals. Also, for both lateral loading types, the axial stiffness degradation and the vertical limit deformation are comparable where collapse occurs at almost the same level of vertical deformation.

Collected experimental data

While some experimental data were the fruit of laboratory tests on specimens already presented in the previous section, some other data were cited by Moehle [1] and summarized in Table 3. The gathered data contains only those of specimens, which went beyond shear failure till they collapsed under vertical loads. The performance of tested columns given in Table 3 varied according to their geometric characteristics, mechanical properties, loading intensity and loading type. Table 4 illustrates some of the obtained results, which were evaluated also as spread results at ultimate limit stage. The collected data from literature and those presented in the previous section are combined in the next steps.

Table 3 Characteristics of tested columns found in literature

Specimen	b (mm)	D (mm)	a (mm)	S_t (mm)	ρ_{ls} (%)	ρ_{ws} (%)	f_{ly} (Mpa)	f_{wy} (Mpa)	F_c (Mpa)	N (kN)
Sezen and Moehle, 2002										
2CLD12	457.2	457.2	1473.2	304.8	2.50	0.17	441.3	468.8	21.1	667.2C
2CHD12	457.2	457.2	1473.2	304.8	2.50	0.17	441.3	468.8	21.1	2668.9C
2CVD12*	457.2	457.2	1473.2	304.8	2.50	0.17	441.3	468.8	20.9	2224.1V
2CLD12M	457.2	457.2	1473.2	304.8	2.50	0.17	441.3	468.8	21.8	667.2C
Lynn and Moehle, 2001										
3CLH18	457.2	457.2	1473.2	457.2	3.00	0.10	330.9	399.9	25.6	502.6C
3SLH18	457.2	457.2	1473.2	457.2	3.00	0.10	330.9	399.9	25.6	502.6C
2CLH18	457.2	457.2	1473.2	457.2	2.00	0.10	330.9	399.9	33.1	502.6C
2SLH18	457.2	457.2	1473.2	457.2	2.00	0.10	330.9	399.9	33.1	502.6C
2CMH18	457.2	457.2	1473.2	457.2	2.00	0.10	330.9	399.9	25.7	1512.4C
3CMH18	457.2	457.2	1473.2	457.2	3.00	0.10	330.9	399.9	27.6	1512.4C
3CMD12	457.2	457.2	1473.2	304.8	3.00	0.17	330.9	399.9	27.6	1512.4C
3SMD12	457.2	457.2	1473.2	304.8	3.00	0.17	330.9	399.9	25.7	1512.4C

Notation similar to Table 1, *all data given for compression cycles

Table 4 Compiled results of tested columns found in literature

Specimen		δ_s (mm)	δ_m (mm)	Q_t (kN)	θ (degree)
Sezen and Moehle, 2002	2CLD12	75.4	147.3	314.9	35.0
	2CHD12	25.9	55.9	359.0	25.0
	2CVD12*	56.6	86.4	300.7	25.0
	2CLD12M	84.6	149.9	294.5	35.0
Lynn and Moehle, 2001	3CLH18	30.5	61.0	271.3	30.0
	3SLH18	29.2	91.4	266.9	30.0
	2CLH18	76.2	91.4	240.2	35.0
	2SLH18	61.0	106.7	231.3	35.0
	2CMH18	30.5	30.5	315.8	25.0
	3CMH18	45.7	61.0	338.1	15.0
	3CMD12	45.7	61.0	355.9	30.0
	3SMD12	45.7	61.0	378.1	25.0

Notation similar to Table 2

ANALYTICAL INVESTIGATION

The seismic performance of reinforced concrete columns beyond their shear failure is investigated in term of maximum lateral deformability. A simple model is assumed at limit stage and when combined to experimental results, it allows a rough evaluation of the lateral deformability that columns may achieve under axial and lateral loadings. This work is intended to be an introduction to future detailed studies.

The analytical method for assessing the lateral drift is based on the shear-friction model suggested by Moehle [1] but modified, herein, by considering dowel action of longitudinal reinforcement bars. This modification resulted in an expression of friction different from the expression proposed by Moehle. While Meohle's expression is a linear function of lateral drift, the expression suggested in the following is a power function of a combination of lateral drift and other intrinsic column's parameters.
The shear-friction model assumes a diagonal failure plane along the column section height. The column would fail by shear after losing some of its lateral strength and reach collapse when it would no more sustain the applied axial load. This stage is considered as an ultimate equilibrium limit and it is attained when the resulting sliding force $\boldsymbol{S}$ (Fig.7) along the failure plane reaches the plane tangent component of the compression force $\boldsymbol{C}$ by mean of total friction $\boldsymbol{\mu}$ (Eq.2). The resulting forces, $\boldsymbol{C}$ and $\boldsymbol{S}$, respectively normal and tangent to the inclined plane are the result of the applied axial load $\boldsymbol{N}$, the action of the force $\boldsymbol{F_{ws}}$ developed by the transverse reinforcement due to tension and the force $\boldsymbol{F_{ls}}$ developed by the longitudinal reinforcement due to dowel action. The vertical action of the longitudinal reinforcement is disregarded due to potential buckling of steel bars. The column's shear strength at the moment of collapse is considered negligible. The assumption on the value of the inclined plane angle $\boldsymbol{\theta}$ has not a negligible effect on the aimed results and very complex to formulate due to the influence of many parameters that are not yet well understood. Assessment of the friction along the presumed failure plane is a function of the forces mentioned previously and expressed by the following relationship.

$$\boldsymbol{S} = \mu\, \boldsymbol{C} \tag{2}$$

where

$$\boldsymbol{C} = \boldsymbol{N}\sin\theta + \left(\boldsymbol{F_{ls}} + \boldsymbol{F_{ws}}\right)\cos\theta \tag{3}$$

and

$$\boldsymbol{S} = \boldsymbol{N}\cos\theta + \left(\boldsymbol{F_{ls}} + \boldsymbol{F_{ws}}\right)\sin\theta \tag{4}$$

By introducing the concrete stress strength F_c, using steel ratios, ρ_{ls} and ρ_{ws}, and steel yield stress strengths, f_{ly} and f_{wy}, respectively, for longitudinal and transverse reinforcements, Equation 2, expressing the required friction at limit equilibrium, is written as follows.

$$\mu = \frac{(1 - K_1)\tan\theta}{K_1 + \tan^2\theta} \tag{5}$$

where

$$K_1 = \frac{\rho_{ws} f_{wy}}{\eta F_c} + \alpha \frac{\rho_{ls} f_{ly}}{\eta F_c} \tag{6}$$

η is the axial load ratio, and
α is a factor counting for the dowel action and including inclination angle parameter. According to the observation made during tests, dowel action is taken as a flexural action at yielding limit of bars considering bar length equal to stirrups spacing.

Even though Equation 5 does not include any variable concerning the lateral displacement at which columns may experience collapse, the formulation will be used counting on experimental test results collected for the purpose of evaluating the ultimate lateral deformability at which columns may lose their ability to sustain vertical loads. Actually, the friction factor is regarded as a variable affected by the lateral deformability as well as some other parameters.

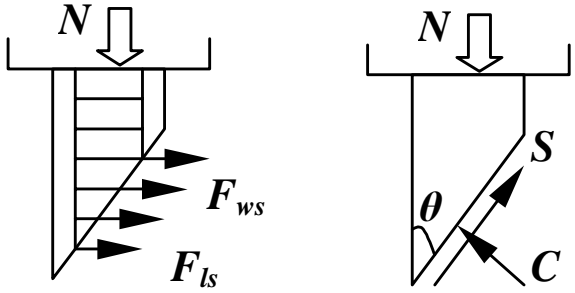

Fig.7 Assumed equilibrium forces for shear model

Friction formulation

As to friction variation, considering or neglecting the dowel action of longitudinal reinforcement resulted in differences as to required friction values that satisfy limit equilibrium at columns' ultimate stage. On the basis of the observed inclination angles on tested specimens, the number of stirrups crossing the main cracks and the formulation given in Equation 5, the required friction, after some trials, was expressed relatively well when dowel action was considered and by combination of different parameters rather than by a single parameter, to name the lateral drift ratio R. The required friction, when dowel action was considered is shown in Fig.8 and expressed by

$$\mu = 0.5\,(k\ R)^{-0.36} \tag{7}$$

where R expresses the attained maximum lateral drift ratio in %, and

$$k = \frac{\rho_{ws}\ f_{wy}}{\eta\ F_c} \tag{8}$$

The formulation in Equation 7 intends to be compared to the formulation given in Equation 5 after expressing Equation 6 in a simple way by means of experimental data. Actually, it was found that Equation 6 might be expressed in terms of transverse reinforcement ratio, concrete strength and axial load ratio, as illustrated in Fig.9. For the range of specimens mentioned herein, Equation 6 is expressed as follows.

$$K_1 = 0.03 + 1.33\,k \qquad (9)$$

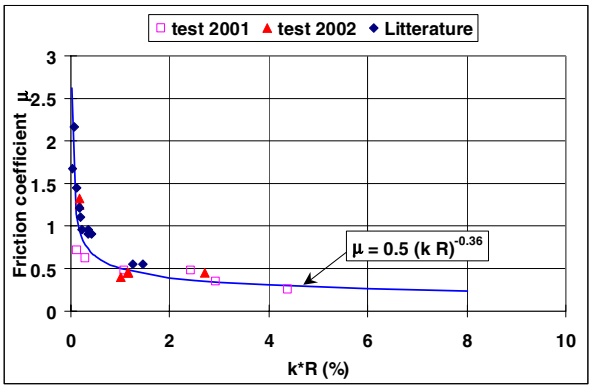

Fig.8 Proposed variation of friction

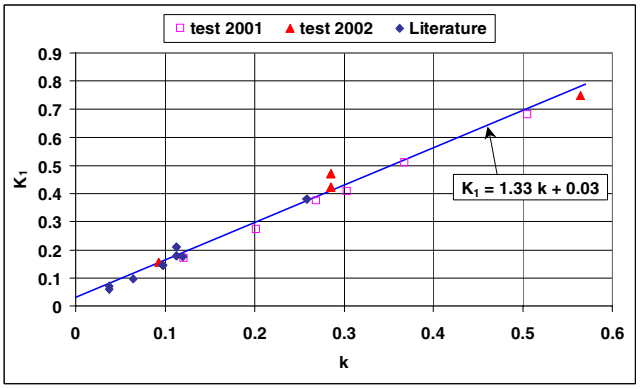

Fig.9 Assumed variation of K_1 factor

Lateral drift evaluation

As it was mentioned previously, inclination of failure plane varied from one specimen to another specimen and was found hard to predict due to implication of different parameters and variables that influences beginning and progress of cracks. Although a trial to formulate the mentioned inclination conveniently could be suggested, the spread data is still of concern. This fact drives the analysis to assume a value that might induce an optimum required friction as higher as possible like given in the following. For actual cases, the parameter K_1 is always positive and when considered as constant, the friction at collapse, computed from Equation 5, would reach its maximum value when $\tan\theta = \sqrt{K_1}$, then

$$\mu_{max} = \frac{1 - K_1}{2\sqrt{K_1}} \qquad (10)$$

The variation of maximum friction, according to the inclination angle and for different values of the parameter k, when Equation 9 is integrated, is illustrated in Fig.10. When only maximums are considered, the line passing through all peaks (maxima curve) is then considered as an upper limit that cannot be overflowed. However, this line is not taken into account when the friction coefficient has negative values, which correspond to inclination angles greater than 45 degrees. Finally, by assuming that the friction assessed by Equation 7 is equal to the friction assessed by Equation 10, the lateral drift R at limit stage can be written in terms of the parameter k as given in Equation 11.

$$R\,(\%) = \frac{1}{k}\left(\frac{0.97 - 1.33k}{\sqrt{0.03 + 1.33k}}\right)^{1/0.36} \qquad (11)$$

Equation 11 is illustrated in Fig.11, which includes also the experimental results. The obtained curve forms a lower boundary for the majority of experimental data involved in this study. While the curve surrounds all experimental data for specimens considered relatively slender with large spacing of stirrups

(data gathered from literature), it does not enclose some experimental data for specimens considered relatively short with closer spacing of stirrups. Although this deficiency, which might be due to omitting to take into account some other influencing parameters, like the effect of lateral loading type in the model, or the effect of the shear span ratio the curve can, roughly, be considered as a limit of the lateral drift that columns might assure under combined axial and lateral loadings. According to the formulation, it suggests that lateral drift increases when parameter ***k*** increases. While this fact is acceptable for a certain range of parameter ***k***, the proposed formulation would be unsatisfactory after a certain value of the same parameter, where the assessed ***R*** value would be far higher than the actual one, as it can be seen for one of the tested specimens ($k \approx 0.5$) in Fig.11. To prevent such case, an upper limit should be fixed from a reasonable level at which no reinforced concrete columns with insufficient stirrups would be expected to perform beyond it. For instance, by referring to the present experimental data, a maximum lateral drift ratio of 9% might be an acceptable limit when the parameter ***k*** reach a value higher than 0.4. However, it is worth to note here that this formulation is based on the assumptions of shear-friction model, where behavior of well-confined columns is not of concern. Limiting the maximum value may be improved in case other new data would be included.

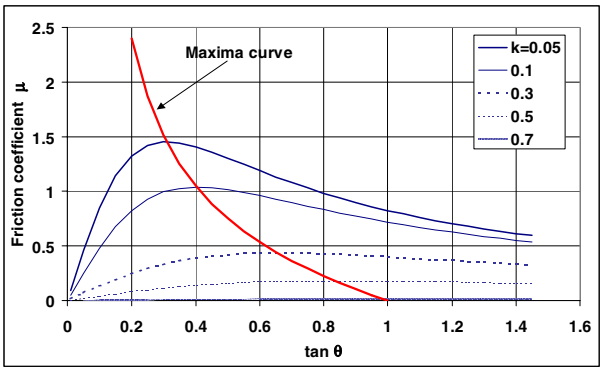

Fig.10 Variation of friction and maxima curve

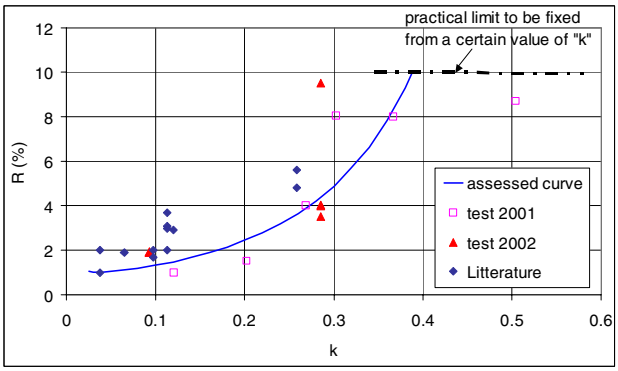

Fig.11 Proposed curve of lateral drift

CONCLUSIONS

Experimental results reached the following conclusions for the tested columns. Under the same lateral loading: the higher axial load is, the steeper is failure plane. The higher axial load ratio is, the lower is lateral deformability. Larger lateral deformability is reached under varying axial loads than under constant axial load. Under the same axial loading: the lower number of hysteretic reversals is, the slightly steeper is failure plane. For high transverse reinforcement ratio or low shear span ratio, few-reversal-loading type induces larger lateral deformability than many-reversal-loading type. However, for low transverse reinforcement ratio lateral loading has a negligible influence on the maximum attained lateral deformability. Experimental results identified that cracking pattern is an important indicator that conditioned failure mode and collapse of columns failing in shear. Also, it is noticed that inclination of failure planes is tremendously random and complex to formulate simply by means of columns characteristics.

A simple shear-friction model has been used to assess the limit lateral drift of reinforced concrete columns, which are insufficiently outfitted transversally with stirrups. The analysis took as basis some experimental data carried by the authors and some other data from literature. In order to ensure, statistically, relatively wide range-samples, various geometric and material characteristics were selected. Also, different loading types, laterally and axially, were applied.

Combining analytical and empirical formulations lead to a rough evaluation of the lateral drift at a stage where columns would not be any more able to sustain applied vertical loads. The lateral drift ratio is evaluated directly as a function of the applied axial load, the concrete strength and the transverse steel content. The action of longitudinal reinforcements is not considered because of a probable buckling of steel bars, however, their dowel action is, indirectly, taken into account. While for some ranges of axial load, concrete strength and transverse steel, the proposed formulation gives satisfaction, for other ranges of the same parameters, the formulation might need to include some other parameters to reach a better conclusion. Probably, by introducing some other parameters like the slenderness of columns or loading type the formulation would be improved significantly.

While this formulation is regarded as a result of a limited number of tested specimens within a certain range of parameters, it cannot be intended as a general to all reinforced concrete columns. More data and more understanding on the behavior of such columns are needed to reach a better assessment of the maximum deformability achieved by reinforced concrete columns at ultimate limit stage.

REFERENCES

1. Moehle J., Elwood K., Sezen H., Lynn A., "Gravity load collapse of reinforced concrete frames during earthquakes." Uzumeri Symposium, American Concrete Institute, Farmington Hills, Michigan, 2002.
2. Takaine Y., Yoshimura M., Nakamura T. "Collapse drift of reinforced concrete columns." Architectural Institute of Japan, Journal of Construction Engineering 2003; No.573: 153-160 (in Japanese).
3. Uchida Y., Uezono Y. "Judging collapse of SRC and RC columns failed by shear." Architectural Institute of Japan, Journal of Construction Engineering 2003; No.566: 177-184 (in Japanese).
4. Ousalem H., Kabeyasawa T., Tasai A., Ohsugi Y., "Experimental study on seismic behavior of reinforced concrete columns under constant and variable axial loadings." Proceedings of the Annual Conference of Japan Concrete Institute 2002, 24(2): 229-234, Tsukuba, Japan
5. Ousalem H., Kabeyasawa T., Tasai A., Iwamoto J., "Effect of hysteretic reversals on lateral and axial capacities of reinforced concrete columns." Proceedings of the Annual Conference of Japan Concrete Institute 2003, 25(2): 367-372, Kyoto, Japan
6. Kwak H.G., Filippou F.C., "Nonlinear finite element analysis of reinforced concrete structures under monotonic loads." Computers and Structures 1997; 65(1): 1-16.